SPIN
Vol. 13, No. 2 (2023) 2340006 (9 pages)

DOI: 10.1142/S2010324723400064

Magneto-Optical Spectroscopy of Nanocomposites $(CoFeZr)_x(Al_2O_3)_{100-x}$

Elena A. Gan'shina*, Alexandr B. Granovsky†, Vladimir V. Garshin‡
and Ilya M. Pripechenkov§
Faculty of Physics
Lomonosov Moscow State University
Moscow 119991, Russia
**eagan@mail.ru*
†*granov@magn.ru*
‡*irving.lambert@mail.ru*
§*priil@yandex.ru*

Alexandr V. Sitnikov
Voronezh State Technical University
Voronezh 394026, Russia
sitnikov04@mail.ru

Mikhail N. Volochaev
Kirensky Institute of Physics
Federal Research Center KSC SB RAS
Krasnoyarsk 660036, Russia
volochaev91@mail.ru

Vladimir V. Ryl'kov¶ and Sergey N. Nikolaev‖
National Research Centre "Kurchatov Institute"
Moscow 123182, Russia
¶*vvrylkov@mail.ru*
‖*niklser@list.ru*

Received 29 December 2022
Accepted 27 February 2023
Published 27 April 2023

We present results of magneto-optical investigations of $(CoFeZr)_x(Al_2O_3)_{100-x}$ film nanocomposites in transverse Kerr effect (TKE) geometry in the spectral range 0.5–4.0 eV and magnetic field up to 3.0 kOe. Nanocomposites were deposited onto a glass-ceramic substrate by ion-beam sputtering. The TKE response at room temperature strongly depends on the wavelength of light, applied magnetic field H and the volume metallic fraction. From the analysis of the field dependences of TKE at different wavelengths, it follows that in the as-deposited samples, the interaction between nanoparticles at $x < 30$ at.% is small and the nanocomposite is an ensemble of

*Corresponding author.

superparamagnetic particles; as x increases to 32 at.%, a superspinglass-type state arises, then, in the vicinity of 34 at.%, along with individual superparamagnetic particles, superferromagnetic regions appear. Long-range ferromagnetic order arises at concentrations x less than the percolation threshold for conductivity $x_{\rm per} = 42.6$ at.%. In the presence of two different magnetic states in the samples, TKE is not proportional to the magnetization. Both the field dependences at near-infrared region and the spectral dependences of TKE change significantly after annealing of the samples, while the changes in the field dependences of the magnetization are almost imperceptibly.

Keywords: Superparamagnetism; superferromagnetism; nanocomposites; magneto-optical spectra.

1. Introduction

The continuous interest in recent years in magnetic nanocomposites of the "ferromagnetic metal–dielectric" type is associated both with the variety of their properties that are promising for practical applications, and with the fact that they can be considered as a convenient platform for studying the properties of disordered systems and interactions in a system of magnetic nanoparticles.[1] One of the important possible applications of these multifunctional materials is their use in high-frequency devices, since in a certain concentration range they simultaneously have high electrical resistivity and magnetic susceptibility.[2,3] It has recently been shown that nanocomposites are promising for the creation of memristors.[4] It has also been proposed to use nanocomposites with a low content of nanoparticles as a material for the dielectric spacer in the tunnel junction of a spin valve to reduce the remagnetizing current density.[5]

At a low concentration of single-domain nanoparticles in the dielectric matrix the interaction of the dipole–dipole type is small, and there is no exchange interaction between them, and therefore the nanocomposite behaves at temperatures above the blocking temperature T_b as an ensemble of superparamagnetic (SP) particles, and below T_b as an ensemble of single-domain ferromagnetic (FM) particles independent of each other. With an increase in the concentration of nanoparticles to $x_{\rm SSG}$, increasing of interaction between nanoparticles leads to the formation of the superspinglass (SSG) state, and then at $x_{\rm SSG} < x_{\rm SF} < x$ superferromagnetic (SF) state with extremely low coercive force.[2] Although the formation mechanisms of these states have not been fully elucidated,[2] they are probably associated with dipole–dipole and exchange interactions through a dielectric matrix with magnetic or nonmagnetic ions dissolved in it. And finally, with a further increase in the concentration, accompanied by an increase in the exchange interaction, a FM long-range order arises. This order can occur even when there is no *physical percolation* (so-called in Ref. 2), that is, when there is no direct contact of the granules, which means that the magnetic percolation threshold $x_{\rm FM}$, the physical percolation threshold $x_{\rm phys}$ and the electrical properties percolation threshold $x_{\rm per}$ can differ from each other. Moreover, the percolation threshold in terms of electrical properties $x_{\rm per}$ differs from the metal–insulator transition threshold $x^6_{\rm MI}$ due to different types of transport properties at $x_{\rm MI} < x < x_{\rm per}$ and $x < x_{\rm MI}$. So the transition sequence looks like $x_{\rm SSG} < x_{\rm SF} < x_{\rm FM} < x_{\rm MI} < x_{\rm per} < x_{\rm phys}$. The identification of a specific state of the system is associated with significant difficulties, which requires the use of various experimental techniques, including X-ray and microscopic studies of the microstructure, measurements of magnetic, magnetotransport properties, the Mössbauer effect, etc. (see, for example, Refs. 2,7 and references therein). Recently, we have shown that the SF state can be determined by studying the magneto-optical (MO) properties, namely, field dependences of MO response at different wavelengths.[8]

In this work, it is shown that the method of MO spectroscopy is an effective tool for studying nanocomposites that complements other methods. It is shown that the MO spectra are extremely sensitive to changes in the magnetic microstructure of the samples during annealing, nanoparticle sizes, and the formation of the SF and FM states. MO spectroscopy of ferromagnets can be carried out using various MO effects in the light reflection and transmission geometries (see Refs. 9–12). We used the transverse Kerr effect (TKE), since this intensity effect in the reflection mode is most convenient for measuring the MO spectra of both metal and dielectric films on substrates. The choice of the nanocomposites $(CoFeZr)_x(Al_2O_3)_{100-x}$ for our

study is determined primarily by the fact that $Co_{45}Fe_{45}Zr_{10}$ is a well studied and quite stable soft magnetic material. Preliminary studies and calculations within the effective medium theory for some specific concentrations revealed a strong change in the parameters and properties of nanocomposites $(CoFeZr)_x(Al_2O_3)_{100-x}$ with varying composition.[13,14]

2. Samples and Experimental Details

The $(CoFeZr)_x(Al_2O_3)_{100-x}$ films with $x = 10$–60 at.% were produced at the growth temperature not exceeding 100°C by the ion-beam sputtering technique onto glass-ceramic substrates using the composite targets of the original design.[1,6] Sputtering was carried out in an Ar atmosphere. The compositions of targets were $Co_{45}Fe_{45}Zr_{10}$ and Al_2O_3. The thickness of the produced samples was about $d = 2.7\,\mu$m. Details of sample fabrication and structural characterization are the same as given in Refs. 1, 4 and 6. Samples for transmission electron microscopy (TEM) studies were prepared in cross-sectional geometry using a Hitachi FB-2100 focused ion-beam system (Japan) followed by polishing with low-energy argon ions using a Leica RES102 setup (Austria). Images of the structure of nanocomposite films were obtained by a Hitachi HT7700 TEM (Japan) at an accelerating voltage of 100 kV. Below, we use metal fraction values x determined by the sputtering conditions.[6] As it was shown in Ref. 6, since a part of magnetic ions and nonmagnetic ions from the target are located not in granules but in nonstoichiometric matrix the composition of FM granules and their fraction differ from the composition of the target and values x calculated from the sputtering rate, correspondingly. For the same reasons, the dielectric matrix is not stoichiometric.

Besides as-deposited samples, we studied also samples annealed at 400°C in a magnetic field $H = 2500$ Oe. The temperature of 400°C and the annealing duration of 30 min were chosen in order to

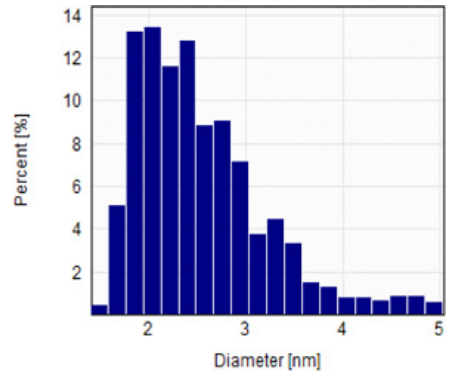

(a) $x = 28.7$ at% as-deposited the average size 2.04 nm

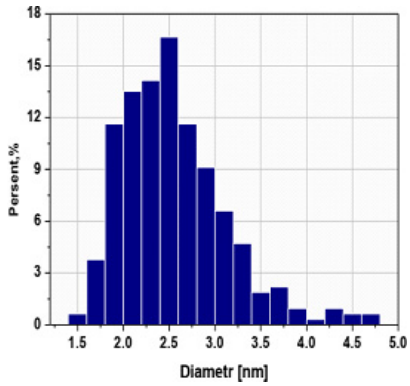

(b) $x = 28.0$ at% annealed the average size 2.55 nm

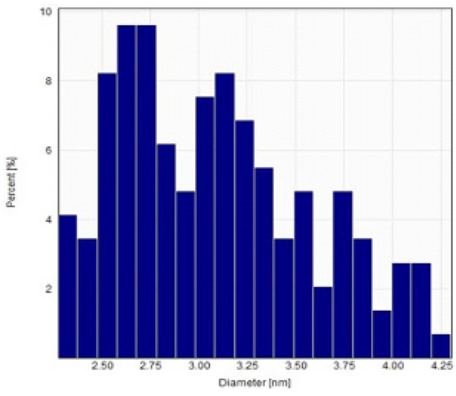

(c) $x = 39.9$ at% as-deposited the average size 3.09 nm

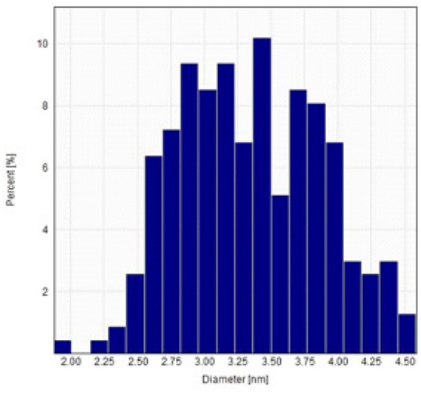

(d) $x = 39.2$ at% annealed the average size 3.35 nm

Fig. 1. Nanoparticle size distribution for nanocomposite $(CoFeZr)_x(Al_2O_3)_{100-x}$: (a), (c) as-deposited samples, (b), (d) annealed samples.

avoid crystallization and oxidation, and at the same time to complete the relaxation processes. The design of the targets and sputtering geometry allows us to get samples with $x = 18$–70 at.% in one cycle. Therefore, for comparison of properties of as-deposited and annealed samples, we used samples with close concentrations obtained in one cycle. The obtained X-ray diffraction patterns indicate that at $x \leq 36.4$ at.% nanogranules are amorphous both in as-deposited state and after annealing. Electron microscopic studies showed that the composites consist of metal granules having round shape and a diameter of 1–5 nm, randomly distributed in the dielectric matrix. The average size and size distribution of nanogranules change with x and after annealing (Fig. 1).

The magnetization measurements were performed using a VSM (Lake Shore 7400).

MO investigations of $(CoFeZr)_x(Al_2O_3)_{100-x}$ film nanocomposites were carried out in the TKE geometry in the spectral range 0.5–4.0 eV and magnetic field H up to 3.0 kOe. We used p-polarized light, the incident angle being $\varphi = 69°$. In the present geometry, the TKE parameter $\delta(\omega, H)$ characterizes the relative change in light intensity $I(\omega)$ at the light frequency ω when the sample is magnetized in the field H

$$\delta(\omega, H) = \frac{I(\omega, H) - I(\omega, -H)}{2I(\omega, H = 0)}. \qquad (1)$$

We used an alternating magnetic field with a frequency of 40 Hz. Two types of measurements were performed for various x at room temperature: field dependences of TKE signal at selected wavelengths and spectral dependences in fixed magnetic field 3.0 kOe. The illuminated part of the film surface was about 0.5 cm^2.

3. Results and Discussions

According to the procedure for determining the percolation threshold x_{per} proposed in Ref. 15, it follows from room temperature measurements of the resistivity that $x_{per} \approx 42.6$ at.%. Annealing changes the grain size distribution and the average grain size (Fig. 1), so that at x around 28 at.% the average grain size increases from 2.09 nm to 2.5 nm and, at x around 39 at.% the average grain size increases from 3.09 nm to 3.35 nm. However, annealing does not lead to noticeable changes in the magnetic properties. As an example, Fig. 2 shows the magnetization curves of samples with $x = 39.9$ at.% before and $x = 39.2$ at.% after annealing. As can be seen from Fig. 2, the changes for two similar compositions are insignificant both for the overall behavior of the curves and for the values H_c of the coercive force. The dependence of the coercive force of the samples on the composition is shown in Fig. 3. The coercive force decreases rapidly with decreasing x and disappears at $x \approx 32$ at.%.

Since rather large domains (regions with predominant orientation of magnetic moments of nanogranules) with a low coercive force are formed in the SF region, and there is no coercive force in the SSG state[2] this concentration can be taken as $x_{SSG} \approx 32$ at.%. This assumption will be confirmed

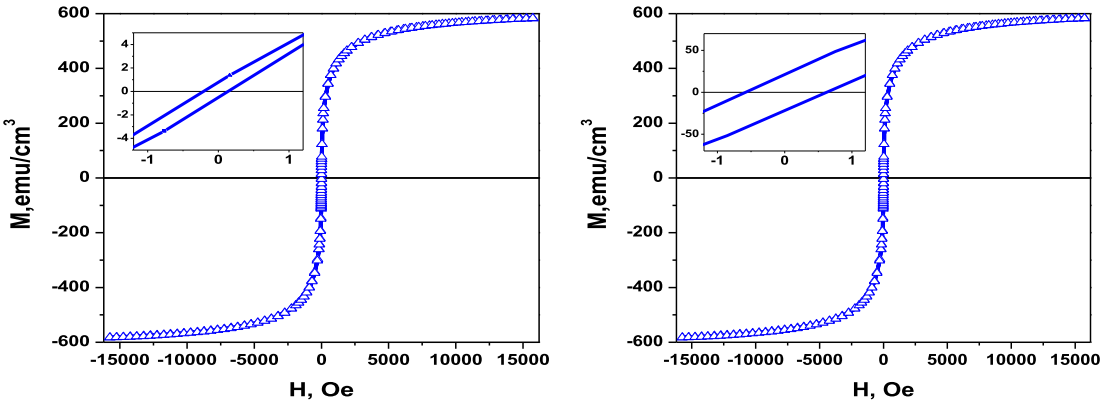

(a) $x = 39.9$ at.% as-deposited (b) $x = 39.2$ at.% annealed

Fig. 2. Field dependences of magnetization for samples (a) as-deposited and (b) annealed. Inset shows hysteresis loops at low fields.

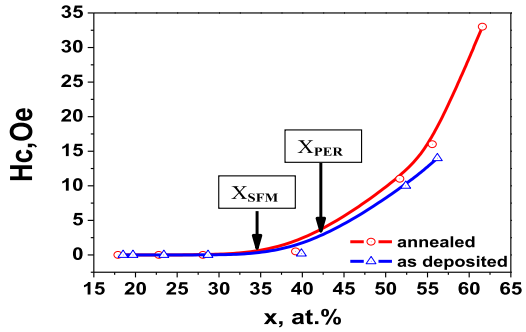

Fig. 3. The coercive force H_c versus the metal concentration x for as-deposited and annealed samples. The percolation threshold x_{per} was determined by transport measurements, x_{SFM} corresponds to the concentration at which SFM state was found by MO measurements (see the text).

below by studying MO response. Since the coercive force is small in both SF and FM states near x_{FM}, it is impossible from these magnetic data to determine the region of existence of SF and the value of x_{FM} that corresponds to the beginning of the formation of long-range FM ordering.

The field dependences of the TKE parameter δ for a number of concentrations of the as-deposited and annealed samples at the selected light quantum energy of 1.97 eV (this choice will be explained below) are shown in Fig. 4, in the form normalized to the maximum signal in Fig. 5, and the spectral dependences in the field $H = 3.0$ kOe in Fig. 6. A number of conclusions follow from the analysis of these figures. First, there is a striking difference between the TKE(H) curves for the as-deposited and annealed samples at $x < 50$ at.%, while the difference in magnetic properties (see Fig. 2) is insignificant.

Second, at a low concentration of nanoparticles, obviously lower than 32 at.%, TKE for as-deposited samples is characterized by a linear field dependence, typical for SP particles, and TKE is negative [Fig. 4(a)]. For annealed samples [Fig. 4(b)], deviations from the linear dependence take place already

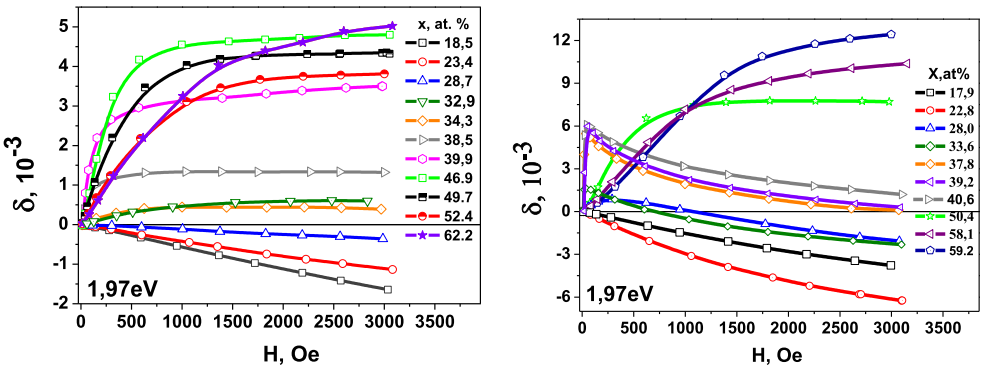

(a) (b)

Fig. 4. TKE field dependences for nanocomposites (CoFeZr)$_x$(Al$_2$O$_3$)$_{100-x}$ for different x: (a) as-deposited, (b) annealed samples.

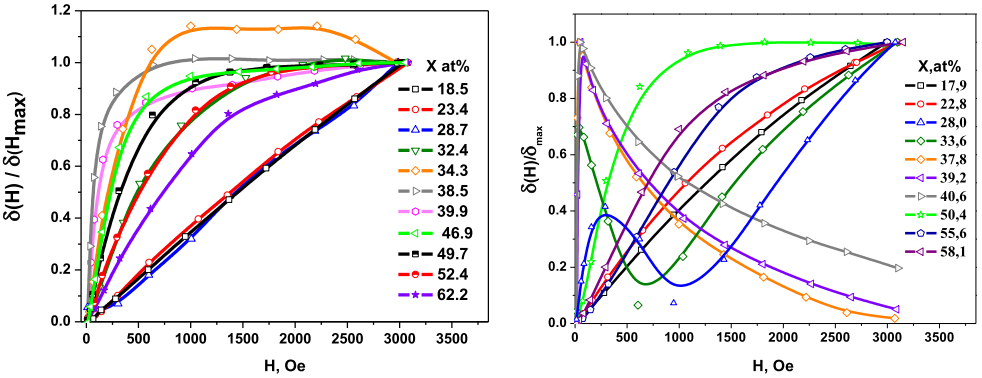

(a) (b)

Fig. 5. Normalized TKE field dependences for nanocomposites (CoFeZr)$_x$(Al$_2$O$_3$)$_{100-x}$ for different x: (a) as-deposited, (b) annealed samples.

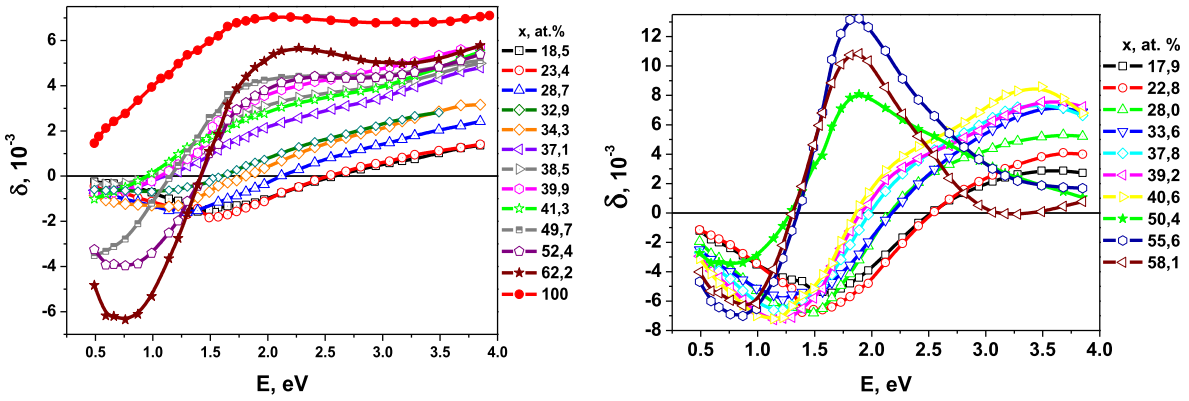

(a) (b)

Fig. 6. TKE spectra for nanocomposites $(CoFeZr)_x(Al_2O_3)_{100-x}$ for different x: (a) as-deposited, (b) annealed samples.

at $x = 18\%$. Third, there is a nonmonotonic dependence of the TKE signal on the metal concentration at $x < 40$ at.%. This nonmonotonicity is especially well seen when the curves are normalized to the maximum signal TKE (Fig. 5). Moreover, the main features of the curves, the sign and field dependence, change in the vicinity of $x = 32$–34 at.%. Fourth, the MO spectrum of nanocomposites differs significantly from the spectrum of the FM component, especially in the near-infrared (IR) region (Fig. 6).

According to the definition of the TKE parameter.[16]

$$\delta(\omega, H) = a(\omega, \varphi, \varepsilon_{xx})\mathrm{Re}\varepsilon_{xy} + b(\omega, \varphi, \varepsilon_{xx})\mathrm{Im}\varepsilon_{xy}, \quad (2)$$

where

$$a(\omega, \varphi, \varepsilon_{xx}) = 2\sin 2\varphi \frac{A}{A^2 + B^2},$$
$$b(\omega, \varphi, \varepsilon_{xx}) = 2\sin 2\varphi \frac{B}{A^2 + B^2}, \quad (3)$$
$$A = \mathrm{Im}\varepsilon_{xx}(2\cos^2\varphi \mathrm{Re}\varepsilon_{xx} - 1),$$
$$B = ((\mathrm{Im}\varepsilon_{xx})^2 - (\mathrm{Re}\varepsilon_{xx})^2)\cos^2\varphi + \mathrm{Re}\varepsilon_{xx} - \sin^2\varphi. \quad (4)$$

$\varepsilon_{xx}(\omega)$ and $\varepsilon_{xy}(\omega)$ are the diagonal and off-diagonal components of the permittivity tensor, respectively. Within the framework of the effective medium theory, these components are complex functions of the optical and MO properties of the components.[13,14,17] For a homogeneous material, the real and imaginary parts are proportional to the magnetization $M(H)$ and therefore $\delta(H) \sim M(H)$. However, for a material containing two different magnetic phases with different field dependences of magnetization, the linear relationship between the TKE parameter and the total magnetization of the sample may be violated. Indeed, let us imagine, for example, that one phase has a high magnetization but a weak MO response, while another magnetic phase with a relatively low magnetization is characterized by a strong MO response, which completely determines the TKE of the sample at the specific light frequency. Such a situation is really the case when the sample contains an easily magnetizing SF or FM phase and hardly magnetizable SP or single-domain particles. Moreover, in the general case of inhomogeneous systems, the imaginary and real parts of the diagonal and off-diagonal components of the permittivity tensor for composites are determined by different functions of the initial parameters of components and therefore can depend differently on the magnetization.

Let us consider the obtained experimental data taking into account these considerations. At a low concentration of nanoparticles in the as-deposited state, the TKE parameter is linear on the field, which was to be expected for an ensemble of noninteracting SP particles in weak and moderate magnetic fields. In this case, the TKE parameter (at $E = 1.97$ eV) is negative for the as-deposited samples at $x \leq 28.7$ at.%. Then, with an increase to 32.4 at.%, the TKE parameter changes its sign and becomes nonlinear [Fig. 4(a)]. There is no hysteresis for this composition (Fig. 3) and the TKE field dependence has nothing to do with the Langevin or the Brillouin function for paramagnetic and SP or SF states [Fig. 4(a)]. Moreover, the amplitude of the TKE parameter of this sample is not less but greater

than that of the composition with $x = 34.2$ at.%, that is with a higher concentration of the magnetic component. All these facts indicate that this sample is neither in SP nor in SF state but in the intermediate magnetic state with strong interaction between grains, which is typical for SSG.[2]

An anomalous behavior of TKE is observed at $x = 34.2\%$, which is clearly seen in Fig. 5(a) when the signal is normalized to its value in $H = 3.0$ kOe. This sample exhibits the coercive force (Fig. 3) and is characterized by the nonlinear field dependence of TKE, which does not follow the Langevin or the Brillouin function and even decreases at $H > 2.0$ kOe [Figs. 4(a) and 5(a)]. This indirectly indicates the formation of the SF state. Additional arguments will be presented below. The field dependence of TKE becomes similar to the Brillouin function type for FM only at $x \geq 38.5$ at.%, that is, we can identify the occurrence of long-range FM order at $x_{\mathrm{FM}} \approx 39\%$.

The choice of wavelength for representing the field dependence of TKE in Figs. 4 and 5 is designed to more explicitly demonstrate the transition from SP to SSG, SF and FM states. Similar curves are observed in almost the entire near-IR region. The magnitude of the signal depends on the particle's size and shape. When the composition changes, the TKE spectrum is transformed (Fig. 6), so for the data in Fig. 4, the type of field dependencies is important, and not the magnitude of the signal, which is why we present normalized data (Fig. 5).

Let us consider in more detail the field dependence of the TKE signal at $x = 34.3$ at.% [Fig. 5(a)]. In the initial section, the signal increases rapidly with increasing field and even exceeds the value at the maximum field, then the signal changes are small, and in a strong field, TKE even decreases [Fig. 5(a)]. This means that there are two magnetic fractions: one is easily magnetized and makes a positive contribution that saturates with increasing field, and the other fraction makes a negative contribution. As noted above when discussing expressions (2)–(4), in this case TKE is not linear in the total magnetization. Since it follows from the data at $x \leq 28$ at.% that the negative contribution at this energy is associated with noninteracting SP particles, we conclude that at $x = 34.2$ at.% there are large SF-type domains, and individual SP particles.

In annealed samples, the field dependences of $\delta(H)$ change significantly [Figs. 4(b) and 5(b)]. The nonlinearity of $\delta(H)$ appears already at $x = 18\%$, but becomes especially pronounced in the concentration range of 28.0–40.6 at.%, where the anomalous behavior of the $\delta(H)$ curves is observed. It is natural to associate it with the change in the average particle size during annealing (Fig. 1). As shown in Fig. 1 during annealing, the average particle size increases and the particle size distribution changes. It is well known that the size and shape of particles have a significant effect on both the optical properties of an ensemble of nanoparticles and the MO parameters of nanoparticles.[13,14] The parameters $\varepsilon_{xx}(\omega)$ and $\varepsilon_{xy}(\omega)$ in expressions (2)–(4) depend on the size and shape of the particles. The reason for this is both the classical size effect due to enhanced electron scattering by nanoparticles interfaces and the plasma frequency shift, that is, these features should be manifested to a greater extent in the near-IR region of the spectrum, which is actually observed from the spectral dependences of TKE (Fig. 6). We also do not rule out that the process of crystallization of nanoparticles begins with increasing particles size during annealing.

The fundamental difference between the TKE in annealed samples in the concentration range of 37.8–40.6 at.%, compared with the as-deposited ones, is a strong decrease in the signal in strong fields, which is seen in both unnormalized and normalized curves [Figs. 4(b) and 5(b)]. Let us consider the anomalous behavior of the field and frequency dependences for a sample with $x = 39.2$ at.% in more detail (Fig. 7). As can be seen from Fig. 7(a), an increase in the field leads to a change in the spectrum, and not just to an increase in the amplitude, and the field dependences of TKE strongly depend on the photon energy [Fig. 7(b)].

The TKE spectrum measured in a relatively weak field $H = 50$ Oe is similar to the TKE spectrum for metallic FM sample CoFeZr [Fig. 6(b)] and has a positive sign in the energy range $E > 1.5$ eV. In this field, not all particles can be even slightly magnetized but only large FM or SF regions. Obviously, the difference between spectra measured at 50 Oe and 3.0 kOe is connected with the MO contribution from small particles or those regions that are not magnetized at 50 Oe. This difference is very similar to the TKE spectra of nanocomposites at small x which are negative at energies below 2.5 eV.

That is, in these samples there are two magnetic phases with contributions of different signs to TKE: a positive contribution for a very easily magnetized SF fraction, and a negative contribution

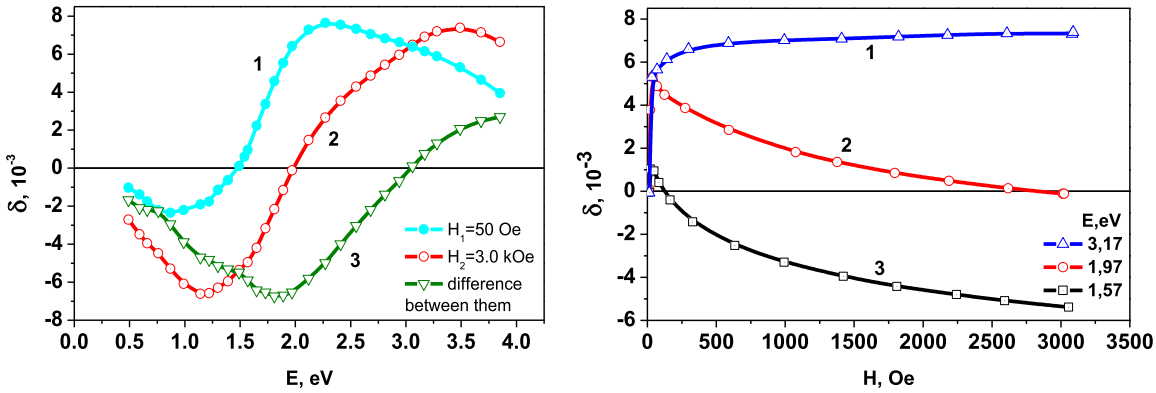

(a) (b)

Fig. 7. TKE spectral and field dependences for annealed sample with $x = 39.2$ at.%: (a) spectra measured in $H = 50$ Oe (1) and 3.0 kOe (2) and the difference between them (3); (b) TKE field dependences at 3.17 eV (1), 1.97 eV (2), 1.57 eV (3).

for individual nanoparticles that are not included in the SF domains. That is, at $x = 28$–40 at.%, we have a situation similar to the behavior of TKE in the as-deposited samples at $x = 34$ at.%, and even more pronounced, since the negative contribution is comparable in magnitude with the positive one, but at higher concentrations. Apparently, annealing led to a shift in all percolation thresholds, both magnetic and transport.

As discussed above, these features are associated with the presence of two magnetic phases with different field dependences of the magnetization $M_1(H)$ and $M_2(H)$ up to the saturation field H_{1s} and H_{2s} for each phase. Therefore, we can rewrite expression (2) in this case as

$$\delta(\omega, H) = \delta_1(\omega)\frac{M_1(H)}{M_1(H_{1s})} + \delta_2(\omega)\frac{M_2(H)}{M_2(H_{2s})}. \quad (5)$$

The parameters δ_1 and δ_2 depend on the concentration x and frequency, but do not depend on the magnetic field, as follows from expression (2). Depending on the frequency, they can be of the same sign or opposite sign. According to the obtained experimental data, in our case they are opposite in sign in the spectral range 1.5–3.0 eV, and therefore, we set $\delta_1 < 0$ and $\delta_2 > 0$. Then, due to the difference between the field dependences $M_1(H)$ and $M_2(H)$ the resulting shape of the TKE spectra will depend on the magnitude of the magnetic field, which explains the data in Fig. 7(a). On the other hand, at a fixed frequency, the field dependence of TKE at $\delta_2 > |\delta_1|$ and the same sign coincides with the field dependence of the TKE parameter of the second component, as in the usual case of a homogeneous ferromagnet, which explains the curve at 3.17 eV in Fig. 7(b); the inverse relation $\delta_2 < |\delta_1|$ corresponds to the curve at 1.57 eV, and intermediate case, when δ_2 and $|\delta_1|$ are of the same order of magnitude, but different sign, corresponds to the curve at 1.97 eV [Fig. 7(b)].

What is the reason for such a strong influence of annealing on the MO properties? With an increase in the average particle size due to the attachment of magnetic and nonmagnetic atoms in the gaps to the granules and the merging of small granules into large ones, on the one hand, their negative MO response should increase, since the previously located magnetic atoms in the gaps did not give an MO response even in strong fields, on the other hand, the effective gap between the granules increases, which leads to an increase in the percolation threshold, and, accordingly, to a shift in the spectral dependences (see Fig. 6), which also leads to an increase in the negative contribution. However, with an increase in the particle size, the contribution to the optical and MO conductivity of the classical size effect decreases. A change in the shape of the granules during annealing also affects the spectrum. Therefore, several factors play a role in the change in TKE during annealing. Calculations within the framework of the effective field theory make it possible to reproduce the shape and amplitude of the TKE spectra,[13,14] but with the selection of several adjustable calculation parameters.

4. Conclusions

MO measurements for $(CoFeZr)_x(Al_2O_3)_{100-x}$ film nanocomposites confirm that with an increase in the metal content, an ensemble of weakly interacting SP

particles transforms into a two-phase magnetic state characterized by the presence of both individual SP particles and SF regions, and then the long-range FM order is formed. The long-range FM order arises at concentrations lower than the percolation threshold for conductivity. In the mixed SF–SP state, TKE is not linear in magnetization. Annealing of the samples leads to significant changes in both the field and spectral dependences of TKE. This is associated with a change in the particle size during annealing. MO spectroscopy demonstrates a higher sensitivity to changes in the microstructure and magnetic state of nanocomposites than magnetometry methods.

Acknowledgments

This work was supported in part by the Russian Foundation for Basic Research under Grant 22-29-00392. Magnetic and MO studies were performed using equipment purchased at the expense of the MSU The authors thank the Krasnoyarsk Regional Center of Research Equipment of Federal Research Center "Krasnoyarsk Science Center SB RAS" for assistance.

References

1. V. V. Ryl'kov *et al.*, *J. Exp. Theor. Phys.* **131**, 161 (2020).
2. S. H. Ohnuma, H. Fujimori, S. Mitani and T. Masumoto, *J. Appl. Phys.* **79**, 5130 (1996).
3. S. Bedanta and W. Kleeman, *J. Phys. D, Appl. Phys.* **42**, 013001 (2009).
4. M. N. Martyshov *et al.*, *Phys. Rev. Appl.* **14**, 034016 (2020).
5. C. N. Gao, Y. X. Yang, Y. Q. Xiong, P. Chen, *J. Phys. D, Appl. Phys.* **47**, 045003 (2014).
6. V. V. Ryl'kov *et al.*, *Phys. Rev. B* **95**, 144402 (2017).
7. A. A. Timofeev *et al.*, *J. Appl. Phys.* **111**, 123915 (2012).
8. E. Gan'shina *et al.*, *IEEE Magn. Lett.* **11**, 2500504 (2020).
9. A. K. Zvezdin, V. A. Kotov, *Modern Magnetooptics and Magnetooptical Materials* (CRS Press, 2020), p. 404.
10. A. V. Malakhovskii *et al.*, *J. Magn. Magn. Mater.* **263**, 161 (2003).
11. Š. Visnovsky *et al.*, *Appl. Phys. Lett.* **100**, 232409 (2012).
12. J. Mistrik *et al.*, *J. Appl. Phys.* **99**, 08Q317 (2006).
13. A. Yurasov *et al.*, *J. Phys., Conf. Ser.* **1389**, 012113 (2019).
14. A. N. Yurasov *et al.*, *Bull. Rus. Acad. Sci., Phys.* **86**, 601 (2022).
15. Y. E. Kalinin *et al.*, *Phys. Solid State* **46**, 2146 (2004).
16. G. S. Krinchik, *Physics of Magnetic Phenomena* (Moscow State University Press, Moscow, 1985) p. 336.
17. E. A. Gan'shina *et al.*, *J. Exp. Theor. Phys.* **98**, 1027 (2004).